Rare Earth Element Geochemistry of the Epembe Carbonatite Dyke, Opuwo Area, North-western Namibia

Ester Kapuka

Geological Survey of Namibia, 6 Aviation Road, Windhoek
<Ester.Kapuka@mme.gov.na>

Abstract :- The Epembe carbonatite dyke was emplaced along a northwest-trending fault zone into syenites and nepheline syenites of the Epembe Subsuite (Epembe-Swartbooisdrift Alkaline Suite). It extends for approximately 6.5 km in a northwest - southeast direction, with a maximum outcrop width of 400 m. The Epembe carbonatite has a Mesoproterozoic age of 1184 ± 10 Ma; field relationships support that it is younger than the enclosing nepheline syenites dated at 1216 ± 2.4 Ma. This study examines geochemical and mineralogical variations within the carbonatite dyke, with special emphasis on rare earth elements (REE). Analytical and petrographic results show that it primarily consists of coarse-grained calcite, with accessory apatite, pyrochlore, aegirine, feldspar and iron oxide, and therefore classifies as calcio-carbonatite. Although the concentration of REE (total REE+Y) in the Epembe carbonatite dyke ranges from 406 to 912 ppm, no REE-minerals were observed in the analysed samples, except for monazite in trace amounts. It is concluded that REE are either contained in accessory minerals, such as apatite and pyrochlore, and/or gangue minerals (e. g. silicates and carbonates). The Epembe carbonatite is enriched in light rare earth elements (LREE) compared to heavy rare earth elements (HREE), which is attributed to fractional crystallisation and chemical substitution primarily affecting former.

Keywords :- Geochemistry, Rare earth elements (REE), Epembe carbonatite dyke

To cite this paper :- Kapuka, E. 2024. Rare Earth Element Geochemistry of the Epembe Carbonatite Dyke, Opuwo Area, Kunene Region, North-western Namibia. *Communications of the Geological Survey of Namibia*, **27**, 19-39.

Introduction

Owing to a globally increased demand, rare earth elements have attracted the attention of numerous exploration companies and researchers to examine potential host rocks, including monazite ± apatite veins, carbonatites, pegmatites, peralkaline igneous rocks, ion-adsorption clays, placers, and certain deep-ocean sediments (Kanazawa and Kamitani, 2006). Currently, most light rare earth elements (LREE) are extracted from carbonatite-related deposits, while heavy rare earth elements (HREE) are mostly derived from REE-bearing ion-adsorption clays (Wall, 2014). Accordingly, carbonatites have become prime exploration targets for junior companies across the globe as they are the principal suppliers of REE and niobium, which are essential raw materials for important economic sectors, such as the manufacture of electric vehicles, permanent magnets and solar panels (European Commission, 2014).

This investigation focuses on the analysis of major and trace elements, including REE, across the Epembe carbonatite, Kunene Region, north-western Namibia, with the aim of establishing and understanding their distribution within the dyke. The study area is situated roughly 95 km northwest of the regional capital Opuwo, between the villages of Ohamaremba and Epembe (Fig. 1).

Regional Geology

The regional geology of the area is characterised by gneisses of the Epupa Metamorphic Complex, intruded by two igneous alkaline suites/complexes, i. e. the Mesoproterozoic rocks of the Kunene Anorthosite Complex with a concordant U-Pb single zircon age of 1370 Ma (Mayer *et al*., 2004) and the Epembe–Swartbooisdrift Alkaline Suite with a

minimum age of 1100 Ma (nepheline syenite and lamprophyre; U-Pb zircon / K-Ar biotite; Menge, 1986); the latter encompasses the Epembe and Swartbooisdrif Subsuites. The metamorphic and igneous units are partly overlain by (meta)-sedimentary rocks of the Neoproterozoic Damara and the Palaeozoic Karoo Supergroup, which, however, in the study area are present only as isolated, transported boulders (Falshaw, 2012). An overview of the intrusive and metamorphic units of the study area is given in Table 1.

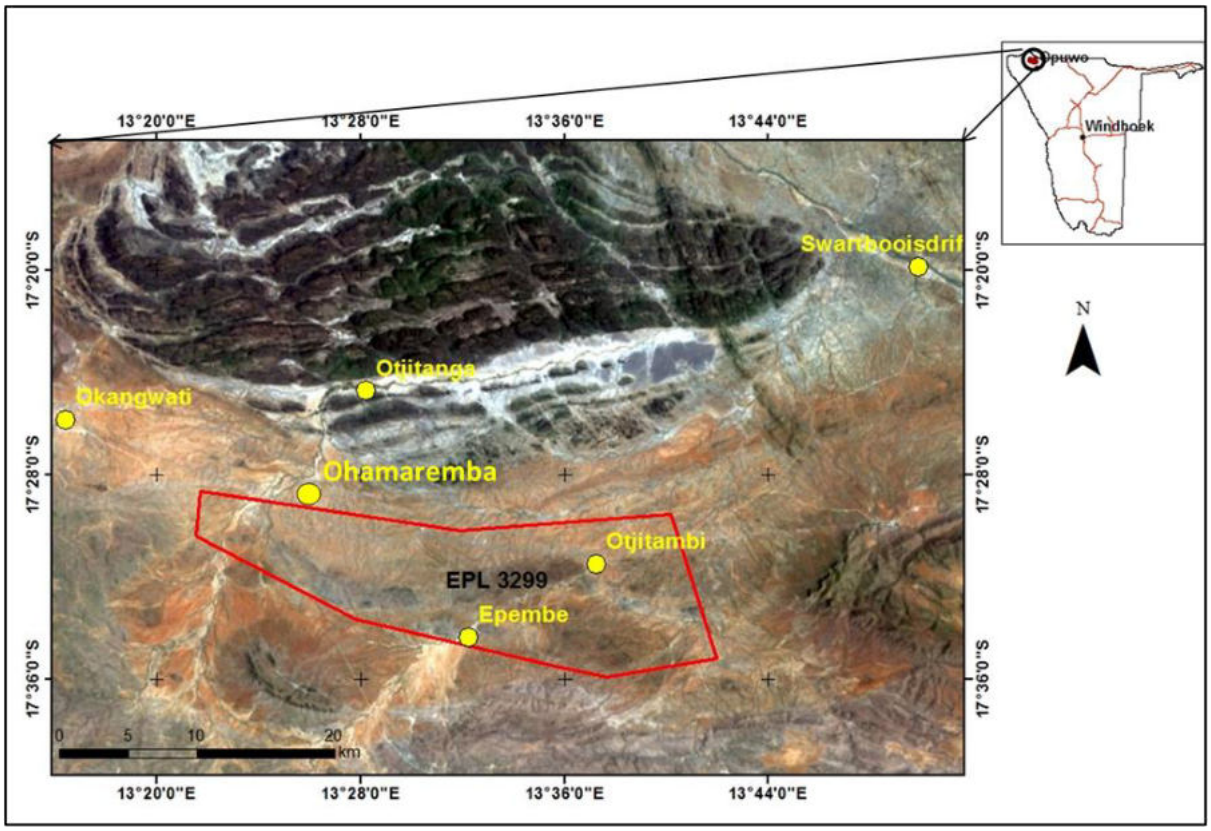

Figure 1. Satellite image (Landsat 8, sharpened) showing the location of the study area and Exclusive Prospecting Licence (EPL) 3299, which covers the Epembe carbonatite dyke (satellite image: National Aeronautics and Space Administration, USA)

Epupa Metamorphic Complex

The metamorphic and igneous rocks of the Epupa Metamorphic Complex (EMC) represent the oldest Palaeo- to Mesoproterozoic basement in the area, which was intruded by the anorthosites of the Kunene Igneous Complex (Maier *et al*., 2008). The EMC is composed of upper amphibolite facies and ultrahigh-temperature granulite facies rocks (Brandt, 2003), which have been subdivided into two distinctive units based on petrology, metamorphic grade, structure, and field relationship (Brandt *et al*., 1999), i. e. the Orue and Epembe units (Fig. 2).

Following the work of Martin (1965) and Köstlin (1967), the Orue unit consists mainly of a widely migmatised volcano-sedimentary sequence, intruded by large volumes of granitic magma. The rocks exhibit uniform upper amphibolite facies metamorphic grade, as well as structural similarities. The Epembe unit encompasses a 50 km long, E-W trending and up to 10 km wide, well-defined terrane of ultrahigh-temperature granulite facies ortho- and paragneisses. The central part of this unit comprises volcano-sedimentary successions of interlayered mafic and felsic granulites, and subordinate migmatitic metasedimentary granulite (Brandt, 2003; Brandt *et al*., 2000, 2007). Both volcano-sedimentary sequences, separated by a subvertical E-W trending fault known as the Otjitambi-Ehomba Fault (Fig. 2), have undergone substantial burial to mid-crustal levels (Brandt, 2003). Subsequently, the Epembe unit was intruded by small stocks and dykes of carbonatite, nephe-

line syenite and lamprophyre of the Epembe Subsuite (Maier *et al*., 2008). While the Orue unit has been dated at 1334 ± 21 Ma (Seth *et al*., 2003), a protolith age of up to 1810 Ma (Drüppel *et al*., 2001; Seth *et al*., 2003) is assigned to the Epembe unit.

Lithology	Intrusive unit	Sub-Unit	Suite/Complex	Age
Carbonatite	Epembe carbonatite, Swartbooisdrift carbonatite		Epembe-Swartbooisdrift Alkaline Suite	
Syenite				± 1100 Ma
Nepheline syenite	Otjitanga-Epembe nepheline syenite			± 1250 Ma
Serpentinite, hornblendite, anorthosite, troctolite	Otjitambi hyperite	Satellite intrusions	Kunene Anorthosite Complex	
Anorthosite	Marginal Zone			
Anorthosite (subordinate olivine anorthosite)	Upper Zone	Zebra Moutains succession		
Troctolite (subordinate anorthosite)	Lower Zone			± 1370 Ma
Granite gneiss, amphibolite			Epupa Metamorphic Complex	± 1470 Ma

Table 1. Stratigraphy of the study area (modified after Menge, 1986, 1996; Seth *et al*., 2003)

Kunene Igneous Complex

The EMC is intruded by the Mesoproterozoic anorthosites of the Kunene Igneous Complex (KIC), which straddles the Namibian/Angolan border, and, with ca. 20 000 km^2, is the largest anorthosite complex of the world (Drüppel, 1999). The southern part of the KIC was first described by Beetz (1933), who established the presence of gabbro, norite, anorthosite and pyroxenite. These rocks were divided into three distinct intrusive successions (e. g. Menge, 1996); 1) massive, light-coloured anorthosite intercalated with 2) dark leucotroctolite - anorthosite in the northwest ("Zebra Mountains"), and 3) a small unit of anorthosite and subordinate, locally olivine-bearing, leucogabbro. The emplacement age of the KIC has been well constrained at around 1370 Ma by various authors (U–Pb single zircon/baddeleyite dating; e. g. Drüppel *et al*., 2007; McCourt *et al*., 2013; Bybee *et al*., 2019).

Swartbooisdrift - Epembe Alkaline Suite

Two successions of alkaline rocks occur in the Epembe – Swartbooisdrift area. The Epembe Subsuite consists mainly of nepheline syenite plugs, the Epembe carbonatite dyke, marginal syenite, and minor syenite and lamprophyre dykes, which intruded Epupa Complex gneisses (Figs 2, 3). Dolerite and quartz dolerite dykes of unknown age are present in the same area and generally follow the same regional trends. The Swartbooisdrift Subsuite, located in the vicinity of Swartbooisdrift on the Namibian/Angolan border, comprises dykes of banded sodalite, analcite, ankerite, cancrinite, albite and magnetite, which intruded mostly Kunene anorthosites and cross-cut older lamprophyres and syenite dykes. The Swartbooisdrift sodalite has been exploited for semi-precious stone and dimension stone.

The Epembe carbonatite dyke, some 40 km southwest of Swartbooisdrift, is distinctly younger than both the anorthosite and the syenites / nepheline syenites. While the latter were dated at 1213 ± 2.5 Ma (Seth *et al*., 2003), a concordant U-Pb age of 1184 ± 10 Ma was obtained for the former (Simon *et al*., 2017); for comparison, the age of the Swartbooisdrift carbonatite has been given as 1140 – 1120 Ma (Drüppel, 2003).

Local geology of the study area

The Epembe carbonatite dyke was emplaced along a northwest-trending fault zone into syenite and nepheline syenites (Menge, 1996); it extends for 6.5 km in a northwest-southeast direction (Figs 3, 4) and dips steeply (70° to 80°) towards the southwest. The

Epembe carbonatite has a maximum outcrop width of 200-400 m; the partially soil-covered dyke is thought to pinch out towards the east-southeast, where it forms several discontinuous veins. The carbonatite dyke is flanked by fenitised metamorphic rocks and alkaline intrusions of shonkinite and nepheline syenite (Fig. 3), with the degree of fenitisation being generally stronger in the fractured and jointed rocks adjoining the intrusions; farther away it becomes more erratic.

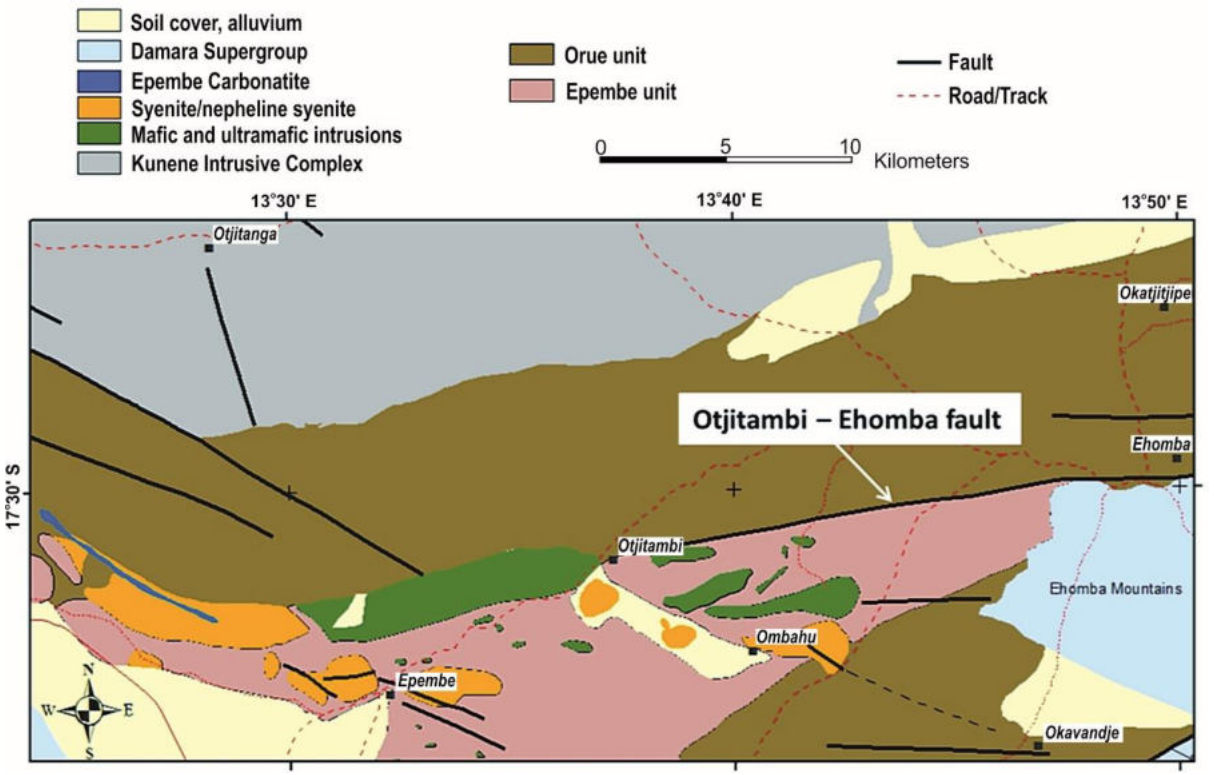

Figure 2. Geological overview of the southern part of the Kunene Intrusive Complex and the adjoining Epupa Metamorphic Complex (after Menge, 1996)

Methodology

Field work was undertaken to study the intrusive relationship between the carbonatites and their host rocks, and to collect representative samples for geochemical and petrographic analysis. Sixteen fresh rock samples (EPB1–EPB16) were collected along the Epembe carbonatite dyke and from the surrounding syenites and fenites (Fig. 5). Hand specimen images (Fig. 6) and thin section photographs (Fig. 7) illustrate mineralogy and texture of rock types present; detailed descriptions are given in Table 2.

A desk top study, including a review of existing publications, maps and miscellaneous documents, such as mineral exploration reports, provided the background for the current investigation. A total of sixteen rock samples was analysed for major and trace elements, and ten carbonatite thin sections, prepared at the Geological Survey of Namibia (GSN) laboratories, were studied to identify component mineral phases. Sample preparation for geochemical analysis was also carried out at the GSN labs. Whole rock samples were crushed to 0.5–15 mm size fraction and milled to a powder finer than 64 microns. A barren quartz flush was pulverised between each sample to minimise the risk of contamination. The sixteen pulp samples were sent to the laboratory of the University of the Witwatersrand (Johannesburg, South Africa) for major and trace element analysis. No control or duplicate samples were analysed due to financial constraints.

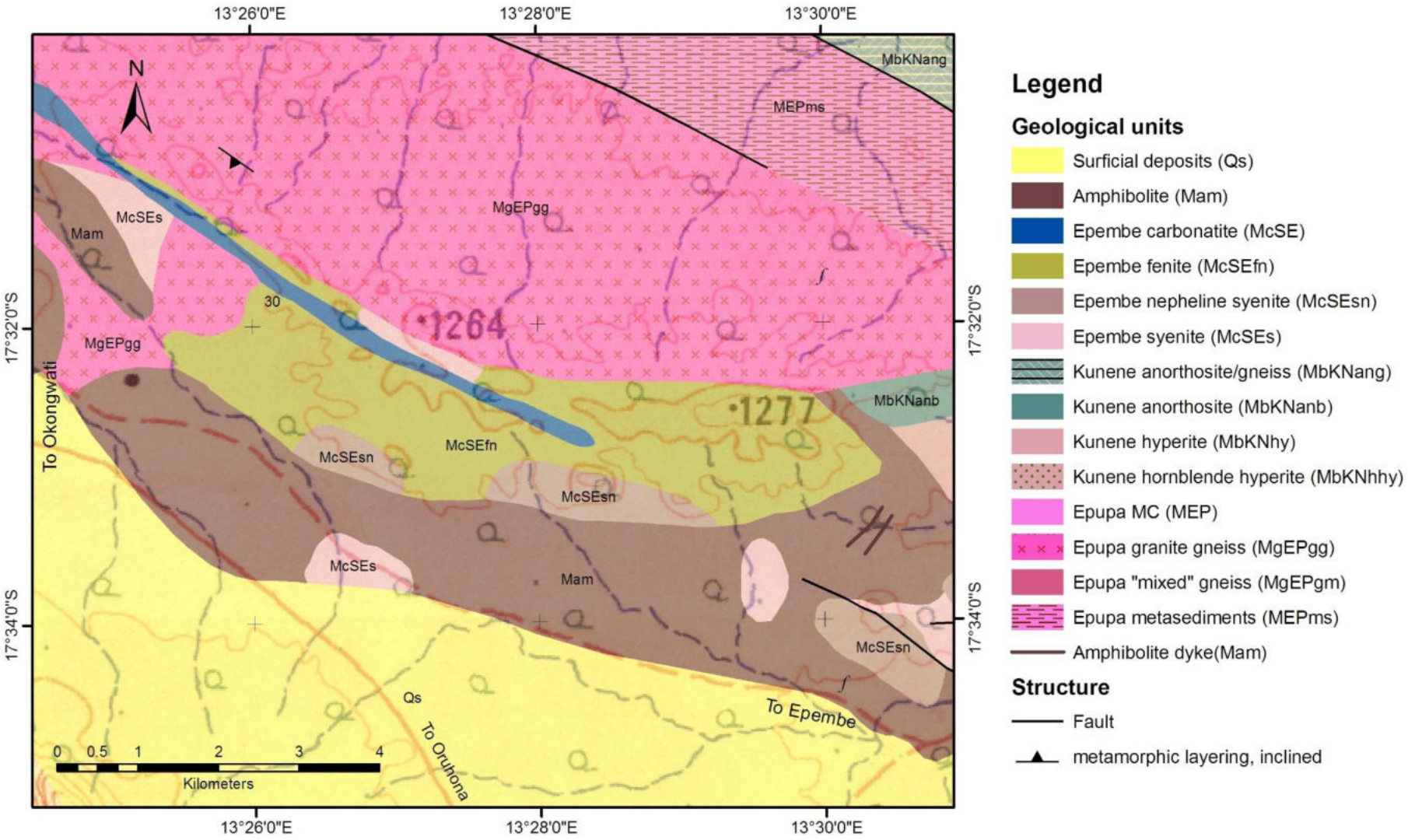

Figure 3. Geological map of the Epembe Subsuite showing the Epembe carbonatite dyke and surrounding rocks (Data source: Menge, 1996)

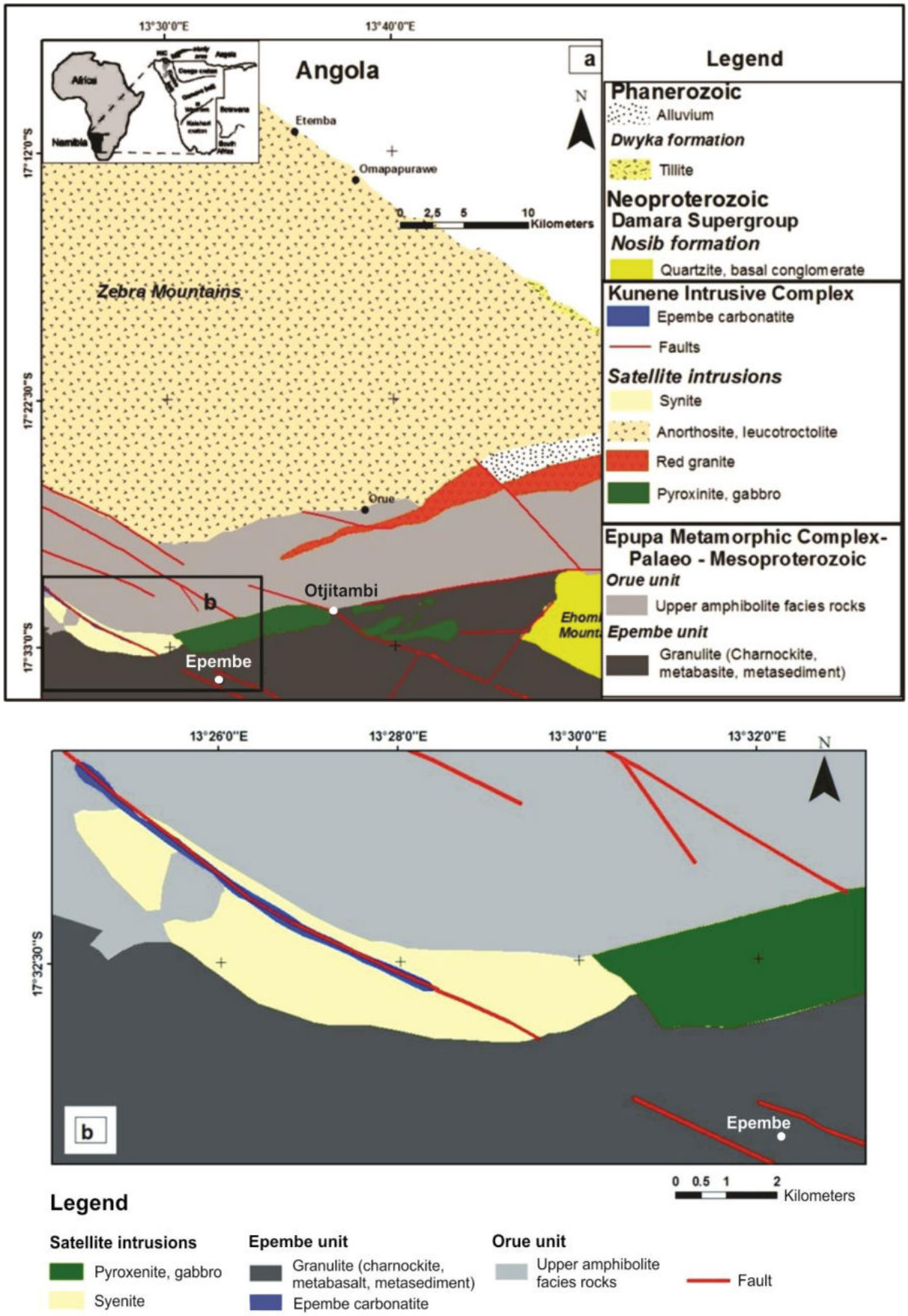

Figure 4. a) Simplified map of part of the Kunene Igneous Complex (KIC) showing location of the study area (black box); b) Sketch map of the study area showing the Epembe carbonatite dyke (after Simon *et al*., 2017)

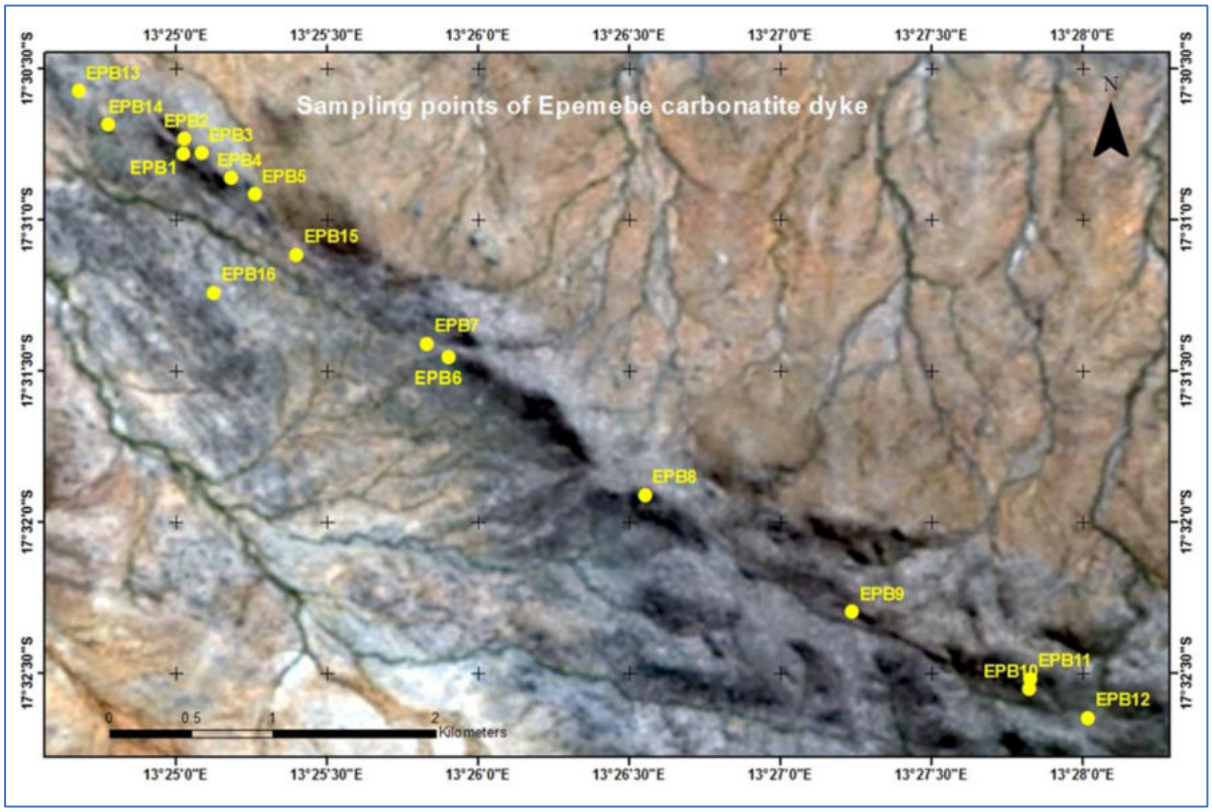

Figure 5. Google Earth image (Landsat 8, sharpened) of the Epembe carbonatite dyke showing sample locations

Major element oxides and trace elements were determined by the Norrish Fusion technique (Norrish and Hutton, 1969); analyses were carried out with a Panalytical (Philips PW2404) X-ray fluorescence spectrometer, using in-house correction procedures. Glass discs for major element analysis were fused with Johnson Matthey Spectrol flux 105 at 1100°C. Sample mass was 0.35 gram and flux mass 2.5 gram. Standard calibration was carried out with synthetic oxide mixtures and international standard rocks as well as in-house controls. Precision is set at 1% for elements making up more than 5% of the mass, and at 5% for elements forming less than 5% of the mass.

Pressed powder pellets for trace element analysis were produced with a Moviol alcohol solution binder. Standardisation was carried out using International Reference Materials of the United States Geological Survey and the NIM (National Institute of Metrology, China) series. Precision was determined based on time counts and is taken as 5% for elements in abundances greater than 100 ppm and 10% for elements in abundances from 10 to 100 ppm.

For rare earth element determination 50 mg of the sample were dissolved with high purity HF-HNO_3 in a MARS microwave digester, before being analysed by ICP-MS (Perkin Elmer DRC-e), using certified primary solution standards. International reference materials AGV-2, BCR-1 and BR-1 were analysed with every run. Agreement to accepted values of the standards was better than 10% for all elements, and often better than 5%.

Mineral identification was carried out on milled rock samples by a Bruker AXS D8 Advance X-ray Diffraction (XRD) Spectrometer. The "Eva" software (Bruker) was employed to identify characteristic peaks of the mineral phases present.

Petrography

The mineralogy of the Epembe Carbonatite-Syenite Subsuite is simple. Major minerals observed are calcite, apatite, biotite, K-feldspar, plagioclase, magnetite and aegirine. Hand specimens from weathered carbonatite outcrops are brown, while fresh surfaces

are a light tan in colour (Fig. 6E). The brown colouration is probably due to ferruginous staining through oxidation. The reddish-brown to white-grey carbonatites show some variation in grain size, ranging from fine- to coarse-grained (0.5 – 5.0 mm); locally the massive rocks are intruded by late-stage hydrothermal calcite veins (Figs 6A & E), which can be observed at outcrop level.

Calcite is the dominant carbonate mineral in all studied samples. Composition varies from almost monomineralic pure calcite (Fig. 6B) to aggregates with accessory apatite, pyrochlore, K-feldspar and minor aegirine, forming interlocking and hypidiomorphic textures. Yellowish-green apatite is found consistently throughout the Epembe carbonatite dyke, making up between 3 to 7 wt. %. Apatite occurs as subrounded or hexagonal, occasionally prismatic, crystals ranging from 0.1 to 2.5 cm in size, which are disseminated throughout the calcite matrix (Fig. 6C). Pyrochlore forms dark-brown, glassy octahedral crystals as well as irregular masses (Fig. 6D). Typically, it is coarse-grained, ranging in size from some tenths of a millimetre to greater than 2 mm. In places the carbonatite is characterised by dark-greenish phlogopite (Mg-biotite) phenocrysts (Fig. 6F). No REE minerals were observed in the Epembe carbonatite samples, except for monazite in trace amounts.

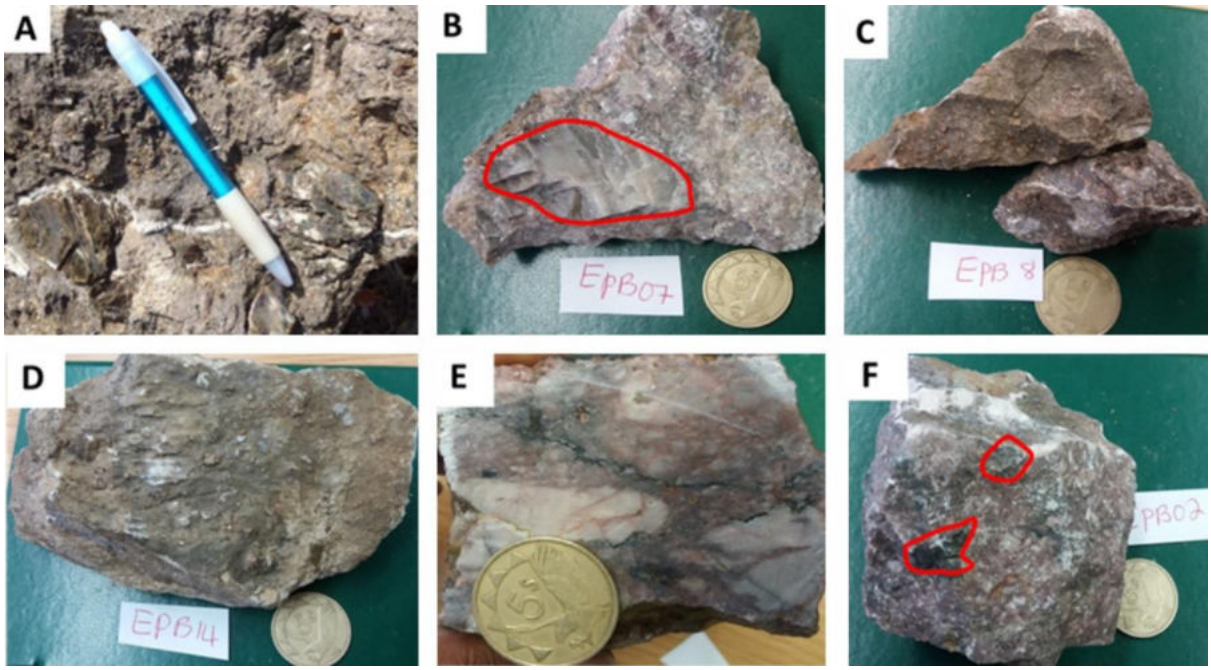

Figure 6. A) Biotite phenocrysts (up to 50 mm) in heavily weathered, feldspar-free carbonatite cross-cut by late hydrothermal calcite veins; B) Coarse-grained calcite crystals (circled in red) up to 5 mm in size; C) Carbonatite sample displaying equigranular, holocrystalline grains of sugary calcite - the pinkish to brownish colour is due to the presence of feldspar and darker minerals including pyrochlore and aegirine; D) Carbonatite sample with dark-brown pyrochlore crystals; E) Fresh carbonatite sample with calcite crystals and late-stage veins stained by iron oxides; F) Medium-grained, pinkish-brown carbonatite with dark-greenish phlogopite (Mg-biotite) phenocrysts (circles); pen = 15 cm, diameter of coin = 25 mm

Ten thin sections were studied with a polarising Carl Zeiss Axiolab microscope under plane- and cross-polarised light to identify main minerals, accessory phases and textures. Confirming field observation and XRD analysis, the most common mineral in the Epembe carbonatite was found to be calcite (~90%), of which two generations are present. In some samples calcite forms large euhedral grains with well-developed cleavages (Fig. 7A), while it is medium- to fine-grained in others (Fig. 7B), possibly reflecting divergent crystallisation histories.

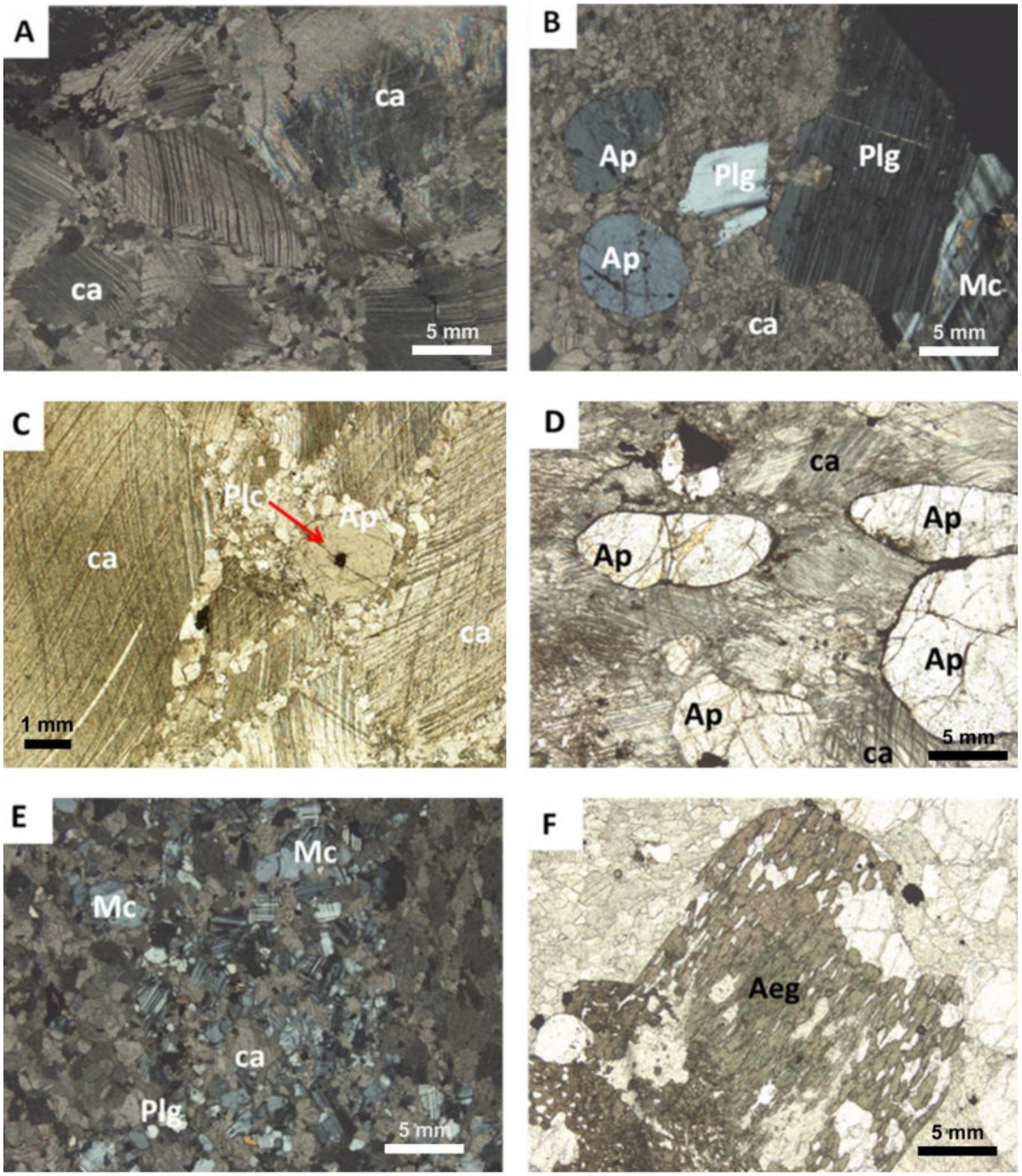

Figure 7. Photomicrographs of representative carbonatite samples in cross- (XPL) and plane-polarised light (PPL): A) EPB01 - coarse-grained calcite with mica filling cracks and fractures (XPL); B) EPB02 - ovoid apatite grains and feldspars embedded in calcite matrix (XPL); C) EPB03 - coarse-grained calcite and ovoid apatite grain enclosing a pyrochlore grain (arrow; PPL); D) EPB08 - elongated and aligned apatite and calcite grains (PPL); E) EPB13 - medium- to fine-grained granular groundmass of anhedral feldspar, interstitial calcite and minor quartz forming an equigranular texture (XPL) of unoriented grains; F) EPB13 - coarse-grained aegirine in calcite matrix (XPL). Abbreviations: Aegirine (Aeg), Apatite, (Ap), Calcite (ca), Microcline (Mc), Pyrochlore (Plc), Plagioclase (Plg)

The second most abundant mineral is apatite, which has been observed in all the studied carbonatite samples. Apatite grains are subrounded to oval and occur in association with pyrochlore, feldspar, calcite and aegirine (Figs 7C & D). Some apatite grains appear elongated and aligned.

Another principal accessory mineral is pyrochlore. The honey-brown to pale yellow mineral occurs as opaque fine- to medium-grained (1µm - 0.5 cm) crystals, especially in veins. Pyrochlore usually is found intricately intergrown with apatite and calcite. Some crystals exhibit zonation, which may indicate a long-lasting crystallisation process within the magma chamber (Wyllie and Biggar, 1966), restricted to late-stage carbonatite magmatism.

Knudsen (1989) describes the development of pyrochlore composition throughout magmatic evolution. During the initial stage of carbonatite magmatism, Ta and Nb are possibly transported as fluoride and phosphate complexes, which explains the common association of apatite with pyrochlore. In places, pyrochlore forms inclusions (Fig. 7C) within apatite crystals showing that pyrochlore formed before apatite.

Micas (mainly biotite and phlogopite) and feldspars (plagioclase – albite, microcline) are found in affiliation with magnetite, hematite and chlorite within the groundmass (Fig.7E) of the carbonatite. They primarily occur in clusters of discrete grains; in places they coat the margins of minerals such as pyrochlore, which identifies them as late-stage crystallisation products. Aegirine forms coarse grains (up to 1 cm) in the calcite matrix (Fig. 7F), and dolomite occurs in minor amounts as fine-grained crystals in veinlets, or as replacement of calcite. Occasionally dolomite coats the grain boundaries of pyrochlore and apatite. Optical characteristics of the observed mineral phases are summarised in Table 2.

Minerals	Texture and Characteristics
Calcite	Coarse-grained calcite is the dominant mineral (~90%). It shows well-developed cleavages (multiple twinning) with high birefringence.
Apatite	Apatite forms white or light-grey to colourless, spherical to subrounded crystals, up to 2.5 mm in size. It is scattered throughout the coarse-grained calcite matrix producing a porphyritic texture.
Pyrochlore	Pyrochlore forms reddish-brown euhedral to subhedral crystals, < 0.2 mm in size, which occur as isolated grains in the calcite matrix. It also occurs as inclusions within apatite.
Feldspar	Feldspar is one of the most common accessory minerals. Colourless plagioclase (albite?) is found in the fine-grained matrix, varying in size from fine-grained in veins to medium-grained.
	Holocrystalline K-feldspar (microcline) occurs within an equigranular groundmass of subhedral, medium- to coarse-grained alkali feldspar.
Mica	Biotite (phlogopite?) forms pale to deep brown or greenish-brown tabular crystals filling interstices between aggregates of other minerals.
Hematite / Magnetite	Rectangular, opaque and cubic grains of iron minerals are observed either in interstices between coarse calcite grains or in the fine-grained matrix.
Aegirine	Where present, aegirine is typically brownish-green in colour, appearing as large (up to 4 mm), aligned phenocrysts either disseminated throughout the matrix or as cumulate concentrations.
Quartz	Quartz occurs rarely either as inclusions within other minerals or as part of the groundmass in association with Fe-bearing minerals and mica.
Chlorite	Where present, chlorite is found in clusters or exploiting fractures.
Dolomite	Dolomite coexists with calcite and is dominant along the margins of opaque minerals.

Table 2. Optical characteristics of minerals identified in the Epembe carbonatite

Geochemistry

Sixteen representative samples of the Epembe carbonatite and adjacent rocks were analysed for major and trace elements including rare earth elements. Major elements were analysed by X-Ray Fluorescence (XRF) and trace elements by inductively coupled plasma mass spectrometry (ICP-MS; see also chapter "Methodology").

Major elements

Major element compositions show high calcium (CaO: 38.01 to 55.31 wt. %), variable iron (FeO: 0.87 to 9.29 wt.% / Fe_2O_3: 0.97 to 10.33 wt%) and low magnesium concentrations (MgO: 0.19 to 1.33 wt. %), which classifies the Epembe samples as calcio-carbonatites and subordinate ferro-carbonatites, on an MgO – CaO – FeO_t (+MnO) ternary diagram (Woolley and Kempe, 1989; Fig. 8). Compared with the global average for calcio-carbonatites (Woolley and Kempe, 1989; Table 3), average Epembe carbonatite shows elevated SiO_2 (4.07 wt. %), and FeO / Fe_2O_3, (2.77 / 3.08 wt. %) concentrations, while MgO (0.40 wt. %) is significantly below average; other elements, including calcium fall within the same range as global averages. Apart from calcite, the Epembe carbonatite contains dolomite [(Ca, Mg $(CO_3)_2$], where randomly substituted magnesium is present in a disordered calcite lattice. Chromium (Cr_2O_3) occurs in trace amounts (<0.025 wt. %; Table 3), and phosphorus is enriched in some of the samples while being depleted in others (compared to the global average; Table 3).

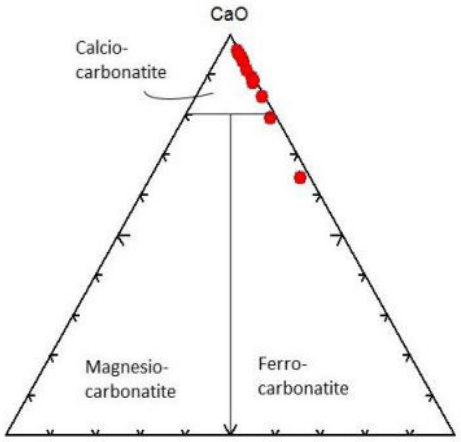

Figure 8. Ternary MgO-CaO-FeOt diagram for carbonatites (after Woolley and Kempe, 1989)

The high proportion of volatiles as evidenced by the high loss on ignition of the Epembe carbonatites (LOI: 28.18 to 41.56 wt. %) is similar to that of average calcio-carbonatites (37.4 wt. %; Table 3). In comparison, fenite and syenite samples only show an LOI of 0.67 wt. % and 3.03 wt. %, respectively. The high LOI in the analysed carbonatite is ascribed to a loss of carbon dioxide (CO_2) during heating.

Sample No	Lithology	SiO_2	Al_2O3	Fe_2O_3	(FeO)	MnO	MgO	CaO	Na_2O	K_2O	TiO_2	P_2O_5	Cr_2O_3	LOI	Total
EPB01	Carbonatite	5.28	1.28	4.41	(3.97)	0.28	0.35	48.98	0.22	0.55	0.13	3.62	0.02	34.71	99.83
EPB02	Carbonatite	3.71	0.52	2.89	(2.60)	0.25	0.23	49.47	0.44	0.19	0.09	2.81	0.02	36.78	97.40
EPB03	Carbonatite	10.89	4.45	10.33	(9.29)	0.25	1.33	38.01	0.21	1.52	1.06	3.43	0.02	28.18	99.68
EPB04	Carbonatite	3.91	1.17	2.25	(2.02)	0.24	0.33	50.00	0.11	0.59	0.14	2.22	0.03	37.14	98.13
EPB05	Fenite	67.81	15.37	3.32	(2.99)	0.05	0.88	1.49	5.10	5.62	0.74	0.32	0.02	0.67	101.39
EPB06	Carbonatite	1.73	0.16	0.97	(0.87)	0.31	0.25	55.31	0.05	0.02	0.03	0.46	0.02	40.83	100.14
EPB07	Carbonatite	1.99	0.52	1.67	(1.50)	0.31	0.23	53.90	0.03	0.15	0.03	0.53	0.02	40.29	99.67
EPB08	Carbonatite	2.62	0.65	1.36	(1.22)	0.29	0.19	51.54	0.01	0.42	0.06	1.18	0.02	39.88	98.22
EPB09	Carbonatite	1.30	0.35	1.18	(1.06)	0.31	0.26	54.69	0.04	0.17	0.03	0.16	0.02	41.56	100.07
EPB10	Syenite	54.57	19.96	2.24	(2.02)	0.07	0.34	4.48	7.01	6.65	0.25	0.37	0.02	4.79	100.75
EPB11	Carbonatite	6.26	1.61	5.83	(5.25)	0.25	0.76	46.18	0.19	0.91	0.33	0.75	0.02	36.08	99.17
EPB12	Carbonatite	2.41	0.79	3.29	(2.96)	0.38	0.59	52.33	0.03	0.36	0.14	2.30	0.03	37.53	100.18
EPB13	Carbonatite	3.42	0.63	3.10	(2.79)	0.29	0.27	49.41	0.34	0.28	0.05	1.50	0.03	38.11	97.43
EPB14	Carbonatite	7.90	2.27	1.55	(1.39)	0.34	0.20	48.83	0.26	1.44	0.03	1.66	0.02	34.41	98.91
EPB15	Carbonatite	1.51	0.50	1.22	(1.10)	0.26	0.19	54.45	0.01	0.15	0.05	0.34	0.02	41.04	99.74
EPB16	Syenite	55.64	20.21	5.73	(5.16)	0.09	1.44	2.73	9.64	1.77	0.62	0.23	0.02	3.03	101.15
Epembe carbonatite	Average	4.07	1.15	3.08	(2.77)	0.29	0.40	50.24	0.15	0.52	0.17	1.61	0.02	37.43	
Calcio-carbonatite	Global average	2.72	1.06	2.25	1.01	0.52	1.80	49.12	0.29	0.26	0.15	2.10	N/A	37.40	

Table 3. Whole rock major element oxides (wt. %) of Epembe rocks and average calcio-carbonatite composition (after Woolley and Kempe, 1989); as major element analyses obtained by XRF cannot provide both Fe_2O_3 and FeO, FeO is taken as Fe_2O_3 x 0.8998 (stoichiometric calculations after Gaillard *et al.*, 2003)

Sample No	EPB01	EPB02	EPB03	EPB05	EPB04	EPB06	EPB07	EPB08	EPB09	EPB10	EPB11	EPB12	EPB13	EPB14	EPB15	EPB16	Epembe carbonatite	Epembe carbonatite	Global Calcio-carbonatite
Lithology	Carbon-atite	Carbon-atite	Carbon-atite	Fenite	Carbon-atite	Carbon-atite	Carbon-atite	Carbon-atite	Carbon-atite	Syenite	Carbon-atite	Carbon-atite	Carbon-atite	Carbon-atite	Carbon-atite	Syenite	Range	Average	Average
Li	1.86	0.49	4.53	6.40	1.37	0.49	1.21	0.75	0.34	8.15	2.01	1.71	0.51	0.77	0.73	46.18	0.3-4.5	1.29	0.1
P	18076.91	11637.61	12778.69	1158.75	8314.23	2024.97	2546.25	5109.31	751.43	1314.42	3516.50	11330.12	7512.34	7694.05	1491.79	1110.54	751.4-18076.9	7137.25	N/A
Sc	4.38	7.03	3.96	4.29	3.66	1.19	0.78	1.77	0.45	0.16	1.86	2.36	6.38	1.51	1.07	1.61	0.45-7.0	2.80	7
Ti	674.36	381.25	5122.76	4018.86	644.72	43.60	137.70	217.33	69.00	863.49	1535.99	600.21	184.22	113.75	144.34	3749.91	43.6-5122.8	759.17	N/A
V	161.81	89.28	116.55	51.45	33.90	2.72	8.25	17.29	5.45	12.07	47.35	28.60	148.95	3.72	19.43	58.22	2.7-161.8	52.56	80
Cr	12.13	9.57	8.32	84.73	6.05	4.62	13.25	3.82	3.96	48.70	8.62	8.45	23.91	10.36	5.34	67.25	3.8-23.9	9.11	13
Co	7.55	3.25	11.47	5.92	4.39	2.64	2.20	4.06	2.19	2.17	7.92	10.62	5.67	4.27	3.44	8.96	2.2-11.5	5.36	11
Ni	19.65	17.75	11.88	7.32	17.32	19.84	21.22	16.59	19.30	3.71	24.07	31.68	21.52	27.21	30.22	11.91	11.9-31.7	21.40	18
Cu	9.27	7.89	7.43	32.45	4.55	9.73	6.29	9.38	3.51	4.24	17.73	19.23	6.88	5.98	4.49	9.82	3.5-19.2	8.64	24
Zn	13.75	12.87	99.36	42.48	15.10	6.71	6.37	518.03	10.57	25.55	59.37	27.73	8.97	54.41	5.99	93.41	6.0-518.0	64.55	188
Ga	12.47	7.06	16.12	22.93	8.22	3.29	3.71	4.66	4.97	28.30	15.18	8.22	6.33	6.63	3.79	27.56	3.3-16.1	7.74	<5
Rb	17.99	6.35	20.90	223.12	20.86	0.99	3.41	7.24	9.58	56.34	77.38	13.53	7.19	21.39	3.72	124.77	1.0-77.4	16.19	14
Sr	4232.20	12315.44	7544.46	444.70	8641.79	5108.84	4538.52	8954.93	5381.32	782.81	8282.47	3354.48	9446.24	7502.44	4832.95	1074.92	3354.5-12315.4	6933.54	N/A
Zr	125.73	99.53	114.13	461.50	94.08	2.61	2.45	116.13	3.07	199.56	224.42	34.96	72.88	6.87	7.64	292.52	2.45-224.4	69.58	189
Nb	1532.57	1090.02	2022.64	20.90	159.58	7.69	40.05	280.70	45.17	26.22	150.53	225.13	64.15	51.78	24.80	141.54	7.7-2022.6	438.06	1204
Ba	96.63	134.62	205.81	2637.84	142.23	53.78	516.21	135.76	110.28	669.35	182.43	saturated	141.36	247.50	98.64	633.98	53.8->LD	172.10	N/A
Sn	18.09	17.93	11.40	2.69	4.23	0.24	1.70	3.68	0.97	0.21	4.62	1.04	16.98	1.44	1.05	3.20	0.2-18.1	6.41	N/A
Cs	0.63	0.24	1.35	3.98	0.71	0.02	0.20	0.07	1.88	1.38	2.95	0.96	0.15	0.12	0.12	5.20	0.02-2.95	0.72	20
Hf	5.04	5.68	3.05	10.62	2.10	0.12	0.13	2.09	0.19	3.56	3.95	0.84	3.59	0.19	0.29	4.96	0.1-5.7	2.10	N/A
Ta	76.50	187.42	367.28	1.15	33.41	0.49	10.76	54.01	8.36	1.13	12.84	48.35	8.42	2.16	3.02	6.43	0.5-367.3	62.54	5
W	0.65	0.12	0.27	0.40	0.19	0.14	0.23	0.12	0.24	0.16	0.37	0.27	0.10	0.22	0.15	0.51	0.1-0.65	0.23	N/A
Pb	5.81	6.74	6.21	27.35	5.02	6.50	2.99	143.84	6.99	2.87	4.76	19.16	7.04	23.24	1.74	11.60	1.7-143.8	18.46	56
Th	21.90	6.37	8.06	72.78	2.08	0.40	0.34	3.22	3.28	0.94	3.05	2.26	0.41	0.76	0.96	4.44	0.3-21.9	4.08	52
U	26.74	331.90	480.06	7.43	25.15	2.18	6.19	67.62	10.67	2.33	6.00	50.28	9.09	1.92	2.10	4.10	1.9-480.1	78.45	8.7

Table 4. Trace element composition (ppm) of Epembe rocks and average calcio-carbonatite (after Woolley and Kempe, 1989; 'calcio-carbonatite' represents samples with CaO/(CaO+MgO+FeOt+MnO) > 80%; N/A= data not available)

Sample No	EPB01	EPB02	EPB03	EPB04	EPB05	EPB06	EPB07	EPB08	EPB09	EPB10	EPB11	EPB12	EPB13	EPB14	EPB15	EPB16	Epembe carbonatite	Epembe carbonatite	Global calcio-carbonatite
Lithology	Carbon-atite	Carbon-atite	Carbon-atite	Carbon-atite	Fenite	Carbon-atite	Carbon-atite	Carbon-atite	Carbon-atite	Syenite	Carbon-atite	Carbon-atite	Carbon-atite	Carbon-atite	Carbon-atite	Syenite	Range	Average	Average
La	176.88	159.36	151.28	166.47	157.42	131.63	123.83	109.64	163.84	13.11	167.19	172.03	133.58	76.81	141.43	26.98	**76.8-176.9**	144.15	608
Ce	347.77	296.86	267.93	307.59	290.66	260.13	241.30	210.87	341.54	32.61	290.23	saturated	257.33	168.92	254.80	53.40	**168.9->LD**	270.44	1687
Pr	39.42	32.69	30.41	33.87	28.65	26.03	26.52	23.07	35.45	2.49	31.95	40.21	29.80	21.57	28.56	6.68	**23.1-40.2**	30.74	219
Nd	159.16	132.66	136.07	136.48	102.65	100.02	112.51	94.82	149.78	10.58	130.90	saturated	128.71	82.44	103.42	27.59	**82.4->LD**	122.25	883
Sm	28.77	23.41	20.86	22.54	15.60	16.18	18.17	17.69	25.30	2.00	20.78	28.64	21.63	17.87	17.80	5.36	**16.2-28.8**	21.51	130
Eu	8.59	6.93	6.14	6.69	3.24	4.51	5.25	5.33	6.90	0.72	6.19	8.59	6.43	5.46	5.00	1.50	**4.5-8.6**	6.31	39
Gd	29.34	24.16	20.80	23.70	12.80	17.95	19.32	19.32	26.83	1.79	21.87	30.04	22.34	18.46	18.21	4.41	**17.6-30.1**	22.49	105
Tb	3.49	2.75	2.28	2.70	1.10	2.20	2.27	2.32	3.04	0.18	2.43	3.52	2.63	2.36	2.07	0.53	**2.1-3.5**	2.62	9
Dy	18.10	14.24	11.17	13.91	4.68	12.35	12.36	13.15	16.08	0.93	12.61	18.10	14.03	12.61	10.50	2.78	**10.5-18.1**	13.78	34
Ho	2.98	2.43	1.82	2.36	0.67	2.29	2.19	2.33	2.80	0.15	2.14	3.10	2.40	2.28	1.86	0.47	**1.8-3.1**	2.38	6
Er	6.78	5.72	4.33	5.70	1.75	5.96	5.49	5.53	6.82	0.37	5.36	7.43	5.76	5.38	4.68	1.22	**4.3-7.4**	5.76	4
Tm	0.93	0.80	0.58	0.79	0.20	0.95	0.85	0.82	0.95	0.05	0.75	1.04	0.83	0.81	0.68	0.19	**0.6-1.0**	0.83	1
Yb	5.66	5.11	3.61	5.07	1.28	6.49	5.63	5.21	6.09	0.30	4.78	6.51	5.16	5.12	4.37	1.26	**3.6-6.5**	5.29	5
Lu	0.77	0.70	0.50	0.72	0.17	0.97	0.81	0.74	0.86	0.04	0.68	0.91	0.74	0.73	0.64	0.19	**0.5-1.0**	0.75	1
Y	83.48	75.31	54.56	72.66	19.44	76.14	70.69	74.33	91.07	3.43	69.77	86.18	67.44	63.28	52.53	10.57	**52.5-91.1**	72.11	119
Total REE + Y	**912.11**	**783.12**	**712.34**	**801.25**	**640.30**	**663.79**	**647.17**	**585.15**	**877.33**	**68.75**	**767.63**	**320.13**	**698.80**	**484.11**	**646.551**	**143.14**		721.41	3850

Table 5: Rare Earth element composition (ppm) of Epembe rocks and average calcio-carbonatite (after Woolley and Kempe, 1989)

Trace and REE elements

Trace and rare earth element results are presented in Tables 4 and 5, respectively. In comparison to fenite and syenite, the analysed carbonatite samples show high concentrations of phosphorus (up to 18076 ppm; EPB01), titanium (up to 5122 ppm; EPB03), strontium (up to 12315 ppm; EPB02) and niobium (up to 2022 ppm; EPB03) (Table 4), while barium exceeds the detection limits of ICP-MS in sample EPB12. Cesium and tungsten are low in the carbonatite samples, with concentrations of < 3 ppm and < 1 ppm, respectively, while other trace elements show moderate concentrations. The high content of phosphorus in sample EPB01 is indicative of the presence of apatite ($Ca_5[PO_4]_3[F, OH]$), while high Ta and Nb concentrations imply an abundance of pyrochlore ($[Na, Ca, Sr, Pb, U]_2 (Nb, Ta, Ti)_2 O_6 (OH, F)$ in samples EPB02 and EPB03.

REE contents of the Epembe carbonatites are high relative to fenite and syenite, though low compared to the global average (Table 5); Ce and Nd in sample EPB12 are above the detection limit of ICP-MS. At the same time, sample EPB12 records the lowest total rare earth (REE_t + Y) concentration of only 406 ppm, while the maximum concentration of 912 ppm occurs in sample EPB01. The total REE content of fenite (640.30 ppm, EPB05) is somewhat lower than that of carbonatites, but significantly higher than in syenite (68.75 ppm in EPB10 and 143.14 ppm in EPB16). The elevated REE content of fenites relative to syenites (Fig. 9, Table 5) is attributed to metasomatic processes, whereby REE constituents were introduced through carbonatitic hydrothermal fluids. Analytical results for REE were normalised to chondrite values (Rock, 1987). Normalised REE values are presented in Table 6 and REE patterns are illustrated in Fig. 9.

REE distribution throughout the Epembe carbonatite dyke exhibits considerable differences, as shown by total REE contents (Tables 5, 6) and chondrite-normalised REE patterns (Fig. 9). The general trend displays a distinct negative (downward) slope from LREE to HREE, demonstrating a strong enrichment of light rare earth elements (LaN/YbN = 10.19 to 28.49) compared to heavy rare earth elements (GdN/YbN = 2.24 to 4.66; Table 6). This is a feature common to most carbonatites, because of the favourable environment they present for the formation of LREE minerals, such as monazite, which has been observed in the Epembe carbonatite, even though only in trace amounts. All samples are characterised by a slight negative Eu anomaly and a positive Gd anomaly.

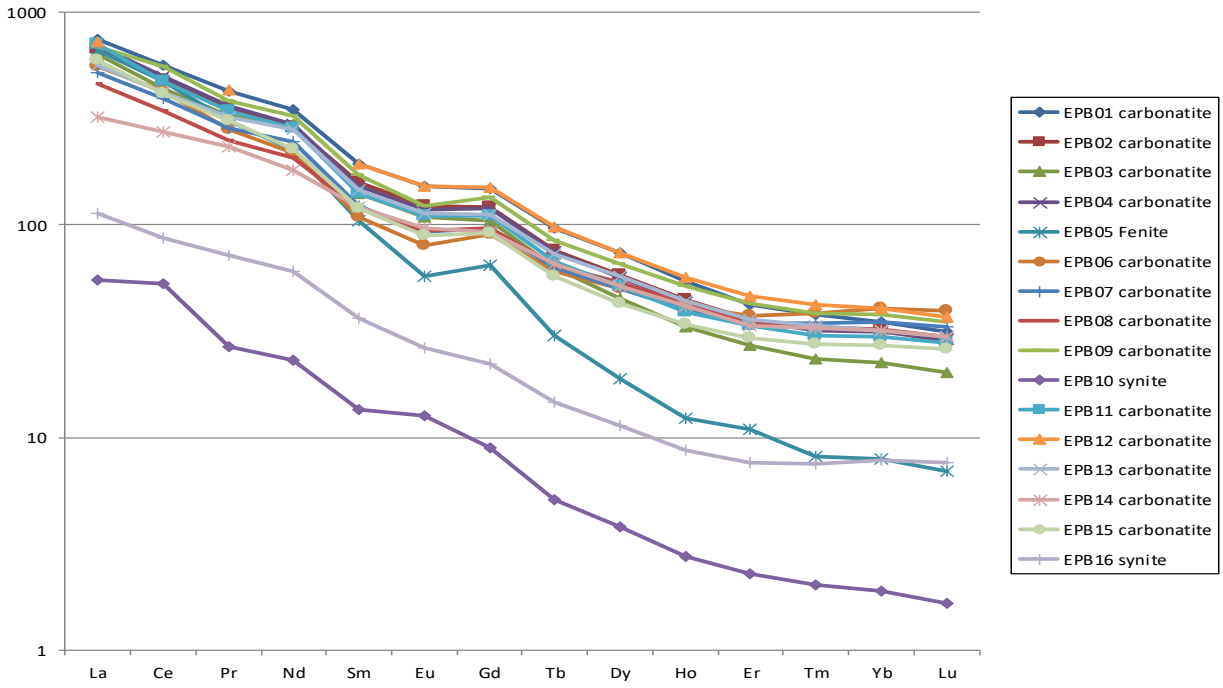

Figure 9. REE patterns for carbonatite, fenite and syenite samples from the Epembe carbonatite dyke and surrounding rocks (chondrite-normalised REE values after McDonough and Sun, 1995)

Sample No	**EPB01**	**EPB02**	**EPB03**	**EPB04**	**EPB05**	**EPB06**	**EPB07**	**EPB08**	**EPB09**	**EPB10**	**EPB11**	**EPB12**	**EPB13**	**EPB14**	**EPB15**	EPB16	Chondrite normalising factors
Lithology	Carbon-atite	Carbon-atite	Carbon-atite	Carbon-atite	Fenite	Carbon-atite	Carbon-atite	Carbon-atite	Carbon-atite	Syenite	Carbon-atite	Carbon-atite	Carbon-atite	Carbon-atite	Carbon-atite	Syenite	
La	746.32	672.41	638.33	702.41	664.20	555.41	522.48	462.63	691.29	55.32	705.46	725.86	563.63	324.10	596.76	113.85	0.237
Ce	567.33	484.27	437.09	501.78	474.15	424.36	393.64	343.99	557.16	53.19	473.46		419.79	275.56	415.65	87.11	0.613
Pr	424.82	352.23	327.74	364.96	308.73	280.52	285.82	248.59	381.95	26.85	344.25	433.32	321.14	232.44	307.79	72.00	0.093
Nd	348.26	290.29	297.74	298.64	224.63	218.85	246.19	207.47	327.75	23.15	286.44		281.65	180.39	226.30	60.37	0.457
Sm	194.36	158.20	140.92	152.32	105.43	109.30	122.76	119.52	170.93	13.50	140.39	193.52	146.16	120.74	120.24	36.23	0.148
Eu	152.52	123.07	109.11	118.81	57.57	80.11	93.20	94.58	122.49	12.70	109.93	152.63	114.14	96.96	88.85	26.55	0.056
Gd	147.44	121.40	104.50	119.12	64.30	90.22	97.08	97.08	134.81	8.97	109.89	150.97	112.24	92.75	91.51	22.17	0.199
Tb	96.65	76.23	63.27	74.65	30.36	60.91	62.74	64.32	84.29	5.07	67.37	97.42	72.96	65.40	57.34	14.76	0.036
Dy	73.56	57.87	45.39	56.55	19.03	50.18	50.25	53.46	65.35	3.79	51.28	73.56	57.02	51.27	42.68	11.32	0.246
Ho	54.56	44.45	33.32	43.26	12.27	41.90	40.02	42.67	51.25	2.77	39.18	56.79	44.03	41.83	34.05	8.66	0.055
Er	42.38	35.75	27.09	35.64	10.91	37.26	34.30	34.56	42.61	2.29	33.47	46.43	36.01	33.64	29.24	7.63	0.160
Tm	37.69	32.43	23.56	32.02	8.14	38.38	34.29	33.24	38.46	2.02	30.16	42.19	33.48	32.71	27.61	7.49	0.025
Yb	35.18	31.74	22.40	31.49	7.93	40.31	34.96	32.33	37.83	1.89	29.68	40.43	32.04	31.81	27.14	7.83	0.161
Lu	31.26	28.33	20.12	29.11	6.95	39.31	33.01	29.88	34.96	1.67	27.80	37.15	29.88	29.80	26.18	7.60	0.025
Total REE	**2952.33**	**2508.66**	**2290.57**	**2560.76**	**1994.59**	**2067.03**	**2050.75**	**1864.34**	**2741.12**	**213.18**	**2448.74**	**2050.28**	**2264.17**	**1609.42**	**2091.34**	**483.58**	**2.510**
Chondrite-normalised ratios																	
Eu/Eu*	0.06	0.05	0.05	0.05	0.04	0.05	0.05	0.05	0.05	0.07	0.05	0.05	0.05	0.05	0.05	0.05	
Ce/Ce*	0.62	0.61	0.58	0.61	0.64	0.66	0.62	0.62	0.66	0.85	0.59		0.60	0.62	0.59	0.59	
LaN/YbN	21.21	21.19	28.49	22.31	83.74	13.78	14.94	14.31	18.28	29.30	23.77	17.95	17.59	10.19	21.99	14.55	
LaN/SmN	3.84	4.25	4.53	4.61	6.30	5.08	4.26	3.87	4.04	4.10	5.03	3.75	3.86	2.68	4.96	3.14	
GdN/YbN	4.19	3.82	4.66	3.78	8.11	2.24	2.78	3.00	3.56	4.75	3.70	3.73	3.50	2.92	3.37	2.83	
LaN/LuN	23.87	23.73	31.72	24.13	95.55	14.13	15.83	15.48	19.77	33.19	25.37	19.54	18.86	10.88	22.80	14.98	

Table 6. REE chondrite-normalised data for sixteen samples of carbonatite, fenite and syenite from the Epembe Subsuite (chondrite values after McDonough and Sun (1995). Chondrite-normalised ratios: Eu/Eu* represents the amplitude of the Eu anomaly [(Eu*=Eu/√(SmN x GdN)], with all carbonatite samples having ratios < 0.07, while Ce/Ce* gives the amplitude of the Ce anomaly [Ce*=Ce/√(LaN x PrN)], with nine samples (including one fenite and one syenite sample) having ratios > 0.6 and the remainder ratios below but close to 0.6; LaN/YbN (=La normalised to chondrite/Yb normalised to chondrite) gives the general steepness of the REE pattern (carbonatite: 10.19 to 28.49; fenite: 83.74); LaN/SmN represents the steepness of LREE (carbonatite: 2.68 to 5.08) and GdN/YbN the steepness of HREE (carbonatite: 2.24 to 4.66).

Discussion and Conclusions

Field relationships indicate that the Epembe carbonatite dyke intruded nepheline syenite of the Epembe Subsuite (Epembe–Swartbooisdrift Alkaline Suite). Contacts between the country rocks and the carbonatite show a very high degree of fenitisation, and blocks of veined, brecciated fenite occur as xenoliths in the carbonatite (Fig. 10). It is assumed that the high temperature of the carbonatite melt caused a mineralogical change in the surrounding country rocks, forming a prominent thermal aureole. Radiogenic age determinations confirm the observed field relationships. While an emplacement age of 1184 ± 10 Ma (U-Pb single zircon; Simon, 2017) was determined for the carbonatite, the nepheline syenites were dated at 1216 ± 2.4 Ma and 1213 ± 2.5 Ma (U-Pb single zircon; Seth *et al*. 2003) and are thus clearly the older.

Figure 10. Xenoliths of syenite within the Epembe carbonatite: A) Syenite xenoliths with NW-SE oriented flow-banding; B) Carbonatite with xenoliths of syenite and aegirine-rich fenite (hammer = 35 cm, pen =15 cm)

Major and trace element geochemistry

The geochemistry of the Epembe carbonatites is consistent with established normal values for carbonatite. Based on the classification system of Gittins and Harmer (1997), which uses the dominant carbonate mineral to categorise carbonatites, the Epembe rocks classify as calcio-carbonatites. Similarly, the chemical classification system of Woolley and Kempe (1989) indicates that the Epembe carbonatites are calcio- or calcite-carbonatites.

The Epembe carbonatites have CaO/ (CaO + MgO + Fe_2O_3 + MnO) ratios of 50.24/ (50.24 + 0.4 + 3.08 + 0.29) = 0.93 on average, which is in agreement with typical calcio-carbonatite with CaO / (CaO + MgO + FeO + Fe_2O_3 + MnO) ratios > 0.8 This classification is supported by petrological studies which show the samples to consist of more than 80% calcite, in accordance with the definition of carbonatite as a rock composed of more than 50% carbonate (Shelley, 1993; Streckeisen, 1979).

Although displaying a certain degree of variation, the whole rock major and trace element composition of the Epembe carbonatites is comparable with the global average for calcio-carbonatites (Woolley and Kempe, 1989; Table 3). While the Epembe carbonatite is characterised by lower-than-average MnO, MgO, Na_2O, V, Cr, Co, Cu, Zn, Y, Zr, Cs and Th (Table 4), the values are still within the global ranges reported for these elements in the literature (e. g. Woolley and Kempe, 1989; Woolley and Church, 2005). Conversely, the Epembe carbonatite shows elevated contents of Li, Ti, Ta, U and Nb in relation to other trace elements (Table 4). Higher than average phosphorus values in some of the samples (Tables 3, 4) are attributed to the local abundance of apatite. Similarly, the high concentrations of tantalum, uranium and, locally, of niobium (EPB01 – 03) indicate the presence of phosphate minerals (pyrochlore and apatite), where uranium can substitute for niobium or tantalum in the mineral structure of pyrochlore, while in the crystal lattice of apatite it substitutes for calcium or phosphate ions. This agrees with exploration results by Kunene Resources, who found the economically inter-

esting rare metals tantalum and niobium contained abundantly in pyrochlore, thus identifying the Epembe carbonatite dyke as a potential Ta-Nb-U deposit (Mariano and Mariano, 2013).

The slightly higher values of CaO and Al_2O_3 in the Epembe carbonatite compared to global average is attributed to the copious presence of calcite, feldspar (microcline) and micas (biotite, phlogopite), respectively, while elevated Fe_2O_3 is due to the occurrence of hematite and magnetite. Finally, low concentrations of K_2O and Na_2O are typical of carbonatites in general.

The new geochemical data show a marked enrichment in critical metals such as niobium and tantalum in the Epembe carbonatite. While these two elements are commonly found together and are chemically similar, they have a very different genesis due to subtle variations in their chemical affinities and the specific conditions under which they form. Both elements are enriched in highly differentiated igneous rocks such as granites, alkali granites, rare metal pegmatites, syenites and carbonatites (Chakhmouradian, 2006). It is concluded that some of the Epembe carbonatites are more fractionated compared to average calcio-carbonatites (Woolley and Kempe, 1989). Elevated silica contents in the Epembe carbonatite (av. ~4 wt% *vs* 2.72 wt. %; Table 3) are related to contamination by the silica-rich, syenitic country rocks, which also occur as xenoliths in the carbonatite.

REE Geochemistry

Total REE concentrations in the Epembe carbonatite range from 406 to 912 ppm (Table 5). REE patterns of Epembe carbonatites resemble each other closely, with a steady decrease from LREE to HREE (Figs 9 and 12), a feature common to most carbonatites (e. g. Jones *et al*., 2013). The Epembe carbonatites, nepheline syenites and fenites display a general enrichment of incompatible over compatible elements, which is reflected by elevated contents of LREE (La-Gd). LREE are more incompatible than HREE and tend to remain in the melt to be incorporated into late-stage (more fractionated) minerals. These may accumulate during the genesis of the carbonatitic melt and subsequent fractional crystallisation (Unger *et al*., 2018). Accordingly, it is assumed that EPB01 is the most fractionated sample, characterised by the highest LREE content (789 ppm), and EPB12 the least fractionated ($LREE_t$ 308 ppm), thus indicating a decrease in fractionation from NW to SE. This is supported by compositional characteristics: while EPB01 displays an intergranular texture of low-temperature minerals such as alkali feldspar and abundant apatite, EPB12 contains more calcite and less feldspar and apatite.

According to Jones and Wyllie (1986), REE, except for Ce and Eu, have a 3^+ valence in most cases. However, in some geological environments, Ce and Eu can have valences of 4^+ and 2^+, respectively, which may lead to anomalous behaviour of these elements relative to other REE. Rollinson (1993) states that europium anomalies are mostly controlled by feldspar in contrast to the trivalent state REE, which are incompatible. The observed negative europium (Eu) anomaly in the Epembe carbonatite indicates the removal of Eu from the magma, with Eu^{2+} substituting for Ca^{2+} in minerals such as plagioclase (both having the same charge and similar radii of 99 vs 107 pm) during fractional crystallisation. While feldspar is retained in the solid residue, a negative Eu anomaly is induced in the melt from which the carbonatite crystallises. A negative europium anomaly is therefore characteristic of REE patterns of late-magmatic carbonatite with Eu^{2+} replacing Ca^{2+} in the crystal lattice of plagioclase, which is stable at temperatures of ≤1000ºC and pressures of < 1 GPa (equalling a depth of less than 30 km; e. g. Wyllie, 1995).

High (La/Yb)N ratios (13 - 29) also show that the Epembe carbonatite is enriched in LREE, which is a general aspect of carbonatites and often related to Sr and Ba enrichment (e. g. Tucker *et al*., 2012). The chondrite-normalised REE pattern of the Epembe carbonatites is comparatively flat in relation to average calcio-carbonatite (Fig. 11). The low absolute and average (721 ppm) REE content of the Epembe carbonatites as compared to the global average for calcio-carbonatites (3850 ppm; Table 5) is attributed to the absence of REE minerals, except rare monazite ([Ce, La, Y, Th] PO_4), in the former.

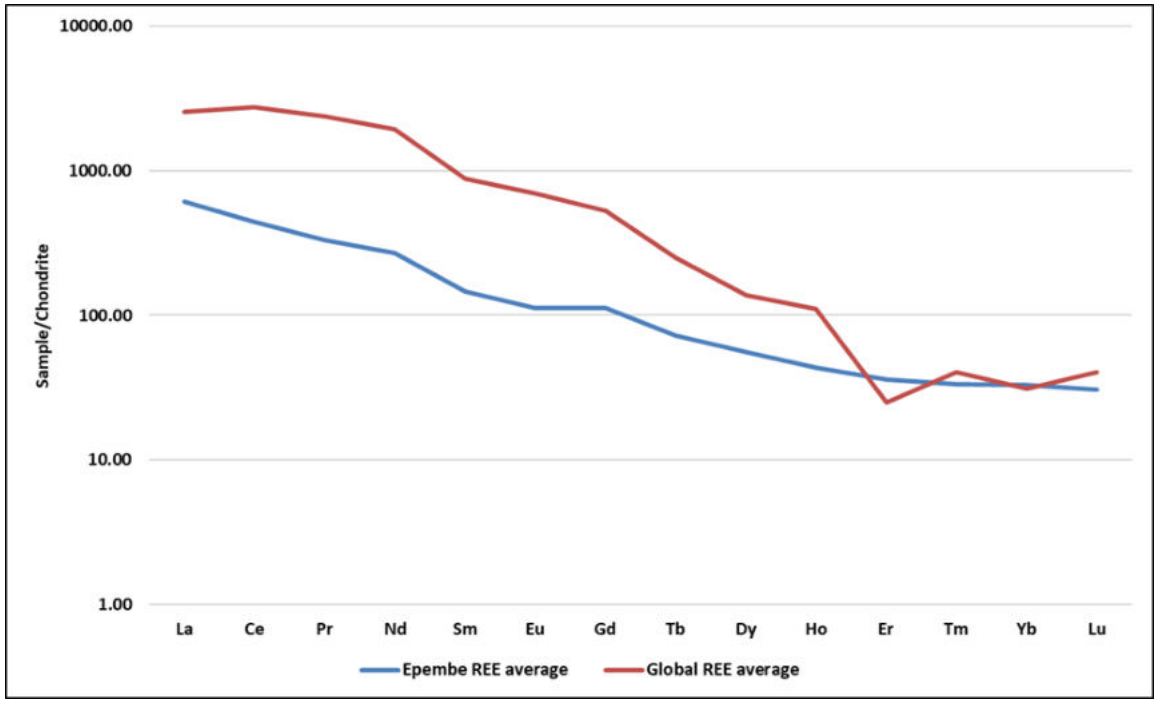

Figure 11. Chondrite- normalised rare earth element (REE) composition of the Epembe carbonatite as compared to global average calcio-carbonatite (after Woolley and Kempe, 1989; chondrite-normalising data from Sun and McDonough, 1995).

REE distribution in Epembe carbonatite

Of all igneous rocks carbonatite has the highest REE content, but their affiliation with specific minerals is less well understood (Kjarsgaard, 1998). Earlier studies of REE distribution (e. g. Kapustin, 1966; Viladkar and Pawaskar, 1989) have established that REE can be strongly enriched in both whole rock and most primary minerals (e. g. calcite, dolomite, pyrochlore, apatite, Ca-silicates). Al Ani *et al*. (2011) state that REE reside mostly in Ca-bearing phases such as apatite ($Ca_5[PO_4]_3[F,OH]$), pyrochlore ($[Na,Ca]_2Nb_2O_6[OH,F]$) and carbonates (e. g. calcite ($CaCO_3$) and ankerite ($Ca\ [Fe,Mg,Mn]\ [CO_3]_2$)), where Ca^{2+} can be replaced by REE cations and / or Sr^{2+}. As no significant REE minerals were found in the Epembe carbonatite, it is assumed that the occurrence and distribution of REE is due to chemical substitution of Ca^{2+} by divalent REE of similar ionic radii.

In carbonatites, REE are mainly concentrated by fractional crystallisation (Chakhmouradian *et al*., 2017; Orris and Grauch, 2002; Williams-Jones *et al*., 2012). At Epembe, the main REE-bearing phases appear to be phosphates and silicates, which are common accessories throughout. REE may also be present in gangue minerals, such as zircon and organic ligands (carbonates), where they can be easily complexed, with trivalent REE acting as electron pair acceptors and ligands donating electron pairs to form coordinate bonds (Edahbi *et al*., 2018).

Whole rock geochemical results are in general agreement with published analyses of apatite and pyrochlore from the Epembe carbonatite-syenite subsuite (Simon *et al*., 2017; Mariano and Mariano, 2013; Unger *et al*., 2018), who concluded that REE are mainly associated with apatite and other phosphates, while Nb and Ta are hosted in pyrochlore.

Acknowledgments

Acknowledgments are due to Kunene Resources (Pty) and the Gecko Exploration team, especially Dr R. Ellmies, for granting permission to work on their EPL, as well as for access to literature and data related to this research project. In addition, I would like to thank Mr Abner Nghoongholoka (GSN) and Mr Iyambo Nekwaya (Gecko Exploration) for their assistance and pleasing company during field work.

References

Al Ani, T., Heikura, P. and Sarapää, O. 2011. *REE-mineralogy and geochemistry of selected drill cores from the southern side of of the Sokli Carbonatite Complex, NE-Finland*. Report of the Geological Survey of Finland, Espoo, Finland, 28 pp.

Beetz, P. F. W. 1933. Geology of South West Angola between Kunene and Lunda Axis. *Transactions of The Geological Society of South Africa,* **36**, 137–176.

Brandt, S. 2003. *Metamorphic evolution of Ultrahigh–temperature granulite facies and upper amphibolite facies rocks of the Epupa Complex, NW Namibia*. PhD Thesis, University of Würzburg, Germany, 285 pp.

Brandt, S., Klemd, R. and Okrusch, M. 1999. Metamorphic evolution of the pre-Pan-African Epupa Complex, Namibia, 23. *Abstracts 31th International Geological Congress,* Rio de Janeiro, Brazil.

Brandt, S., Klemd, R. and Okrusch, M. 2000. Evidence for Ultrahigh – temperature metamorphism in the Pre – Pan-African Epupa Complex, NW Namibia. *Abstracts Geoluanda 2000*, Luanda, Angola, 33-34.

Brandt, S., Will, T. M. and Klemd, R. 2007. Ultrahigh-temperature metamorphism and anticlockwise PT-paths of sapphire-bearing orthopyroxene-sillimanite gneisses from the Proterozoic Epupa Complex, NW Namibia. *Precambrian Research*, **153**, 143-178.

Bybee, G. M., Hayes, H. Owen-Smith, T. M., Lehmann, J., Ashwal, L. D., Brower A. M., Hill, C. M., Corfu, F. and Manga, M. 2019. Proterozoic massif-type anorthosites as the archetypes of long-lived (≥ 100 Myr) Magmatic systems—new evidence from the Kunene Anorthosite Complex (Angola). *Precambrian Research*, **332**, https://doi.org/10.1016/j.precamres.2019.105393.

Chakhmouradian, A. R. 2006. High-field-strength elements in carbonatitic rocks: geochemistry, crystal chemistry and significance for constraining the sources of carbonatites. *Chemical Geology*, **235**, 138–160.

Chakhmouradian, A. R., Reguir, E. P., Zaitsev, A. N., Couëslan, C., Xu, C., Kynický, J., Mumin, A. H. and Yang, P. 2017. Apatite in carbonatitic rocks: Compositional variation, zoning, element partitioning and petrogenetic significance. *Lithos,* **274**, 188–213.

Drüppel, K. 1999. *Petrologie und Geochemie von Anorthositen des Kunene-Intrusiv-Komplexes, NW Namibia*. Diplom Thesis, University of Würzburg, Germany, 224 pp.

Drüppel, K. 2003. *Petrogenesis of the Mesoproterozoic anorthosite, syenite and carbonatite suites of NW Namibia and their contribution to the metasomatic formation of the Swartbooisdrif sodalite deposits*. PhD thesis, University of Würzburg, Germany, 345+199 pp.

Drüppel, K., Littmann, S., Romer, R. and Okrusch, M. 2001. Fenitizing Processes Induced by Ferrocarbonatite Magmatism at Swartbooisdrif, NW Namibia. *Journal of Petrology*, **46**, 377–406.

Drüppel, K., Littmann, S., Romer, R. L. and Okrusch, M. 2007. Petrology and isotope geochemistry of the Mesoproterozoic anorthosite and related rocks of the Kunene Intrusive Complex, NW Namibia. *Precambrian Research*, **156**, 1-36.

Edahbi, M., Plante, B., Benzaazoua, M., Kormos, l. and Pelletier, M. 2018. Rare Earth Elements (La, Ce, Pr, Nd, and Sm) from a Carbonatite Deposit: Mineralogical Characterization and Geochemical Behavior. *Minerals*, **8(2)**, 55, https://doi.org/10.3390/min8020055.

European Commission. 2014. *Report on critical raw materials for the EU*. http://ec.europa.eu/enterprise/policies/raw-materials/files/docs/crm-report-on-critical-raw-materials_en.pdf.

Falshaw, S. 2012. *The Geology and Rare Metal Metallogenesis of the Epembe Carbonatite dyke, North West Namibia*. MSc. Thesis, University of Exeter, Camborne School of Mines, Penryn, UK, 126 pp.

Gaillard, F., Pichavant, M. and Scaillet B. 2003. Experimental determination of activities of FeO and Fe_2O_3 components in hydrous silicic melts under oxidizing conditions. *Geochimica et Cosmochimica Acta,* **67**, 4389-4409.

Gittins, J. and Harmer R. E. 1997. What is ferrocarbonatite? A revised classification. *Journal of African Earth Sciences,* **25**, 159-168.

Jones, A. P. and Wyllie, P. J. 1986. Solubility of rare earth elements in carbonatite magma indicated by the liquidus surface in $CaCO_3Ca(OH)_2La(OH)_3$ at 1 kbar pressure. *Applied Geochemistry*, **1**, 95-102.

Jones, A. P., Genge, M. and Carmody, L. 2013. Carbonate Melts and Carbonatites. *Reviews in Mineralogy and Geochemistry*, **75**, 289-322.

Kapustin, Y. l. 1966. Geochemistry of Rare Earth Elements in carbonatites. *Geochemistry International*, **3**, 1054–1064.

Kanazawa, Y. and Kamitani, M. 2006. Rare earth minerals and resources in the world. *Journal of Alloys and Compounds*, **408**, 1339-1343.

Knudsen, C. 1989. Pyrochlore Group Minerals from the Qaqarssuk Carbonatite Complex. *In*: Möller, P., Černý, P., Saupé, F. (Eds) *Lanthanides, Tantalum and Niobium. Special Publication of the Society for Geology Applied to Mineral Deposits*, **7**, Springer, Berlin-Heidelberg, 80-99.

Kjarsgaard, B. A. 1998. Rare earth elements in sövitic carbonatites and their mineral phases. *Journal of Petrology*, **39**, 2105-2121.

Köstlin, E. C. 1967. *The geology of part of the Kunene basic complex, Kaokoveld, South-West Africa*. M. Sc. Thesis, University of Cape Town, South Africa, 92 pp.

Maier, W. D., Teigler, B. and Miller, R. McG. 2008. The Kunene Anorthosite Complex and its satellite intrusions. *In*: Miller, R. McG. (Ed.). *The Geology of Namibia*, **Vol. 1**, chapter 9, 18 pp. Geological Society of Namibia, Windhoek.

Mariano, A. N. and Mariano A. 2013. *A Preliminary mineralogical study of selected rocks from the Ta-rich carbonatite occurrences, Epembe complex, Namibia*. Confidential Report for Kunene Resources, 91 pp.

Mayer, A., Hofmann, A. W., Sinigoi, S. and Morais, E. 2004. Mesoproterozoic Sm-Nd and U-Pb ages for the Kunene Anorthosite Complex of SW Angola. *Precambrian Research*, **133**, 187-206.

Martin, H. 1965. The Precambrian geology of South West Africa and Namaqualand. *Bulletin of the Precambrian Research Unit*, **161**, University of Cape Town, South Africa, 159 pp.

McCourt, S., Armstrong, R. A., Jelsma, H. and Mapeo, R. B. M. 2013. New U–Pb SHRIMP ages from the the Lubango region, SW Angola: insights into the Palaeoproterozoic evolution of the Angolan Shield, southern Congo Craton, Africa. *Journal of the Geological Society, London*, **70**, 353–363.

McDonough, W. F. and Sun, S. S. 1995. The Composition of the Earth. *Chemical Geology*, **120**, 223-253.

Menge, G. F. W. 1986. Sodalite-carbonatite deposits of Swartbooisdrift, South West Africa/Namibia. *In*: Anhaeusser, C.R. and Maske, S. (Eds) *Mineral deposits of Southern Africa*, **Vol. 2**. Geological Society of South Africa, Johannesburg, 2261-2268.

Menge, G. F. W. 1996. The eastern portion of the Kunene complex, its satellite intrusions and the alkaline suite between Epembe and Swartbooisdrif, Kaokoland, South West Africa. Unpublished report, Geological Survey of Namibia, 128 pp.

Norrish, K. and Hutton, J. T. 1969. An accurate x-ray spectrographic method for the analysis of a wide range of geological samples. *Geochimica et Cosmochimica Acta*, **33**, 431–453.

Orris, G. J. and Grauch, R. I. 2002. Rare Earth Element Mines, Deposits and Occurrences. U.S. Geological Survey, *Open File Report*, 02-189, USA, 174 pp.

Rock, N. M. S. 1987. The need for standardization of normalized multi-element diagrams in geochemistry: a comment. *Geochemical Journal,* **21**, 75-84.

Rollinson, H. R. 1993. *Using geochemical data: Evaluation, presentation, interpretation*. Longman Scientific and Technical Press, Routledge, London, 384 pp.

Seth, B., Armstrong, R. A., Brandt, S., Villa, I. M. and Kramers, J. D. 2003. Mesoproterozoic U-Pb and Pb-Pb ages of granulites in NW Namibia: reconstructing a complex orogenic cycle. *Precambrian Research*, **126**, 147-168.

Shelley, D. 1993. *Igneous and Metamorphic rocks under the microscope. Classification, textures, microstructures and mineral preferred orientations*. Chapman and Hall, London, 445 pp.

Simon, S. J. 2017. The *Epembe Niobium-Tantalum Deposit, NW Namibia. U-Pb Age and Resource Estimation*. M. Sc. Thesis,

China University of Mining and Technology, Xuzhou, China, 96 pp.

Simon, S. J., Wei, C. T., Ellmies, R., Yang, H., and Soh Tamehe, L. 2017. New SIMS U-Pb age on zircon from the Epembe carbonatite dyke, NW Namibia: Implications for Mesoproterozoic evolution of carbonatites at the southern margin of the Congo Craton. *Journal of African Earth Sciences*, **135**, 108-114.

Streckeisen, A. L. 1979. Classification and nomenclature of volcanic rocks, lamprophyres, carbonatites, and melilitic rocks: Recommendations and suggestions of the IUGS subcommission on the systematics of igneous rocks. *Geology*, **7**, 331–335.

Tucker, R. D., Belkin, H. E., Schulz, K. J., Peters, S. G., Horton, F., Buttleman, K. and Scott, E. R. 2012. A major light rare earth element (LREE) resource in the Khanneshin Carbonatite Complex, southern Afghanistan. *Journal of Economic Geology*, **207**, 197-205.

Unger, G., Zimmermann, R. and Gloaguen, R. 2018. 3D-Modeling of the Epembe (Namibia) Nb-Ta-P-(LREE) Carbonatite Deposit: New Insights into Geometry Related to Rare Metal Enrichment. *Minerals*, **8(12)**, 600; https://doi.org/10.3390/ min8120600.

Viladkar, S. G. and Pawaskar, P. B. 1989. Rare earth element abundances in carbonatites and fenites of the Newania complex, Rajasthan, India. *Bulletin of the Geological Survey of Finland*, **61**, 113-122.

Wall, F. 2014. Rare earth elements. *In*: Gunn, G. (Ed.), *Critical Metals Handbook*. John Wiley and Sons, Hoboken, New Jersey, 312-339.

Williams-Jones, A. E., Migdisov, A. A. and Samson, I. M. 2012. Hydrothermal mobilisation of the rare earth elements: A Tale of "Ceria" and "Yttria". *Elements*, **8**, 355–360.

Woolley, A. R. and Kempe, D. R. C. 1989. Carbonatites: nomenclature, average chemical compositions, and element distribution. *In*: Bell, K. (Ed.) *Carbonatites - Genesis and Evolution*. Unwin Hyman, London, 1-14.

Woolley, A. R. and Church, A. A. 2005. Extrusive carbonatites: A brief review. *Litho*s, **85**, 1–14.

Wyllie, P. J. 1995. Experimental petrology of upper-mantle materials, processes and products. *Journal of Geodynamics*, **20**, 429–468.

Wyllie, P. J. and Biggar, G. M. 1966. Fractional crystallization in the "carbonatite systems" CaO-MgO-CO_2-H_2O and CaO-CaF_2-P_2O_5-CO_2-H_2O. *In*: *Papers and Proceedings of the 4th General Meeting, International Mineralogical Association*. I.M.A. Volume, Mineralogical Society of India, 92-105.